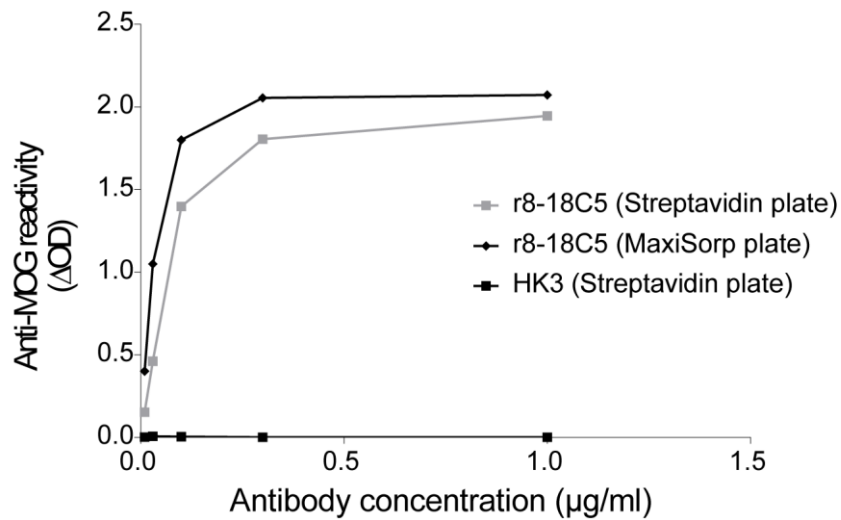
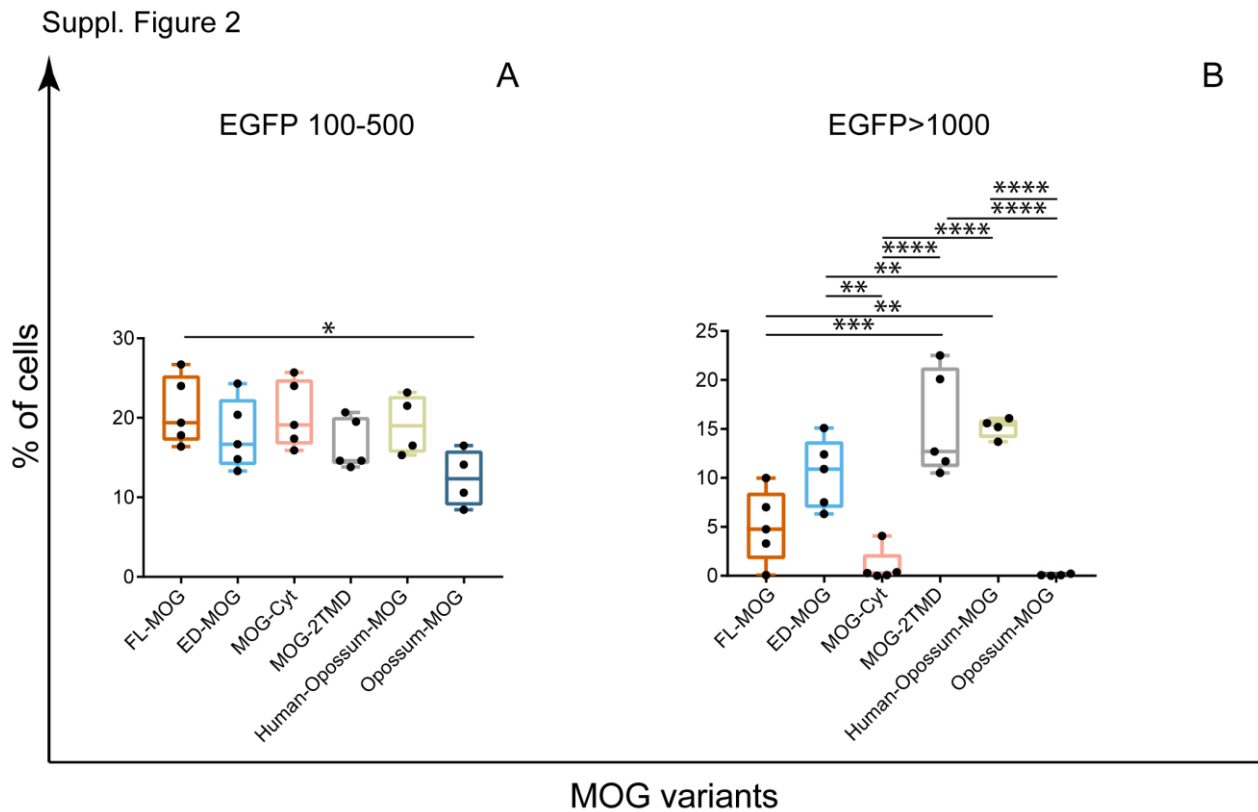


Suppl. Figure 1



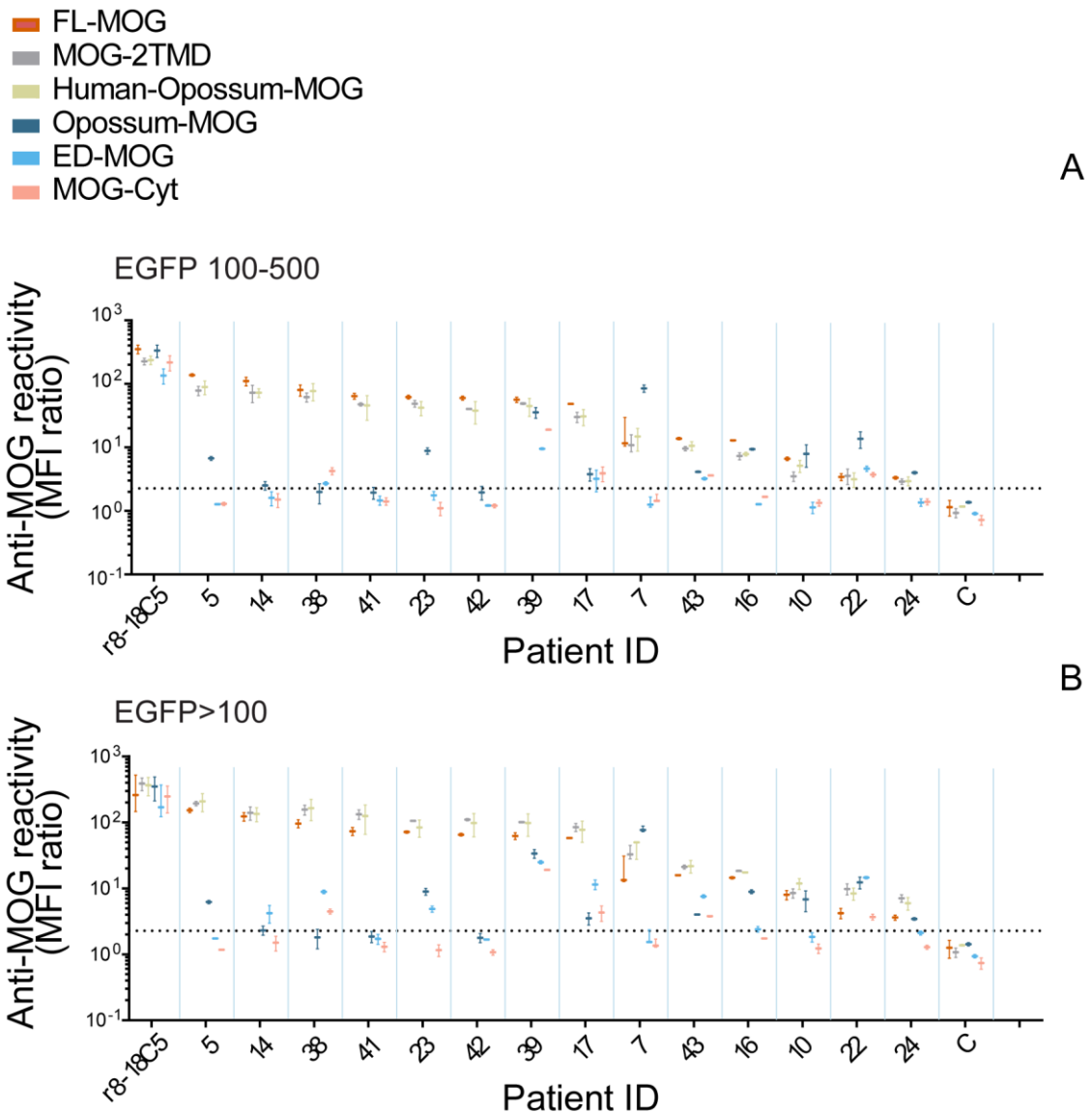
Suppl. Figure 1: Validation of the MOG ELISAs with r8-18C5. MOG-1-125 was bound to MaxiSorp plates and delta OD was calculated by subtracting the OD of BSA coated MaxiSorp plates (black rhombus). Alternatively, MOG was biotinylated at its C-terminal Avi-tag and bound to streptavidin plates and delta OD was determined by subtraction of streptavidin coated wells (grey square). Binding of the MOG-specific r8-18C5 and the control mAb HK3 was compared. The control mAb HK3 is shown for the Streptavidin plate. The background level of this control mAb was similar on the MaxiSorp plate (not shown).



Suppl. Figure 2: Different intensity of expression of MOG-variants after transfection.

HeLa cells were transiently transfected with the indicated MOG-variants, which were all expressed as a fusion protein with EGFP. After 24h, the intensity of expression of the transfected variants was assessed by measuring the EGFP signal by FACS. The raw data is shown in the dot-plot in **Figure 4**. Here, the percentages of cells with EGFP signals of 100-500 (**A**) and >1000 (**B**) are displayed. Error bars indicate SEM of 4-5 replicates. When the gates are set to EGFP 100-500 (**A**) all the constructs have a similar expression. Only FL-MOG is significantly more expressed than opossum-MOG ($p < 0.05$). **B**) When the gates are set to include only the highest expressing cells (EGFP >1000), the different intensities of expression are revealed. The intensity of expression was calculated using one-way ANOVA Tukey's multiple comparisons statistical test.

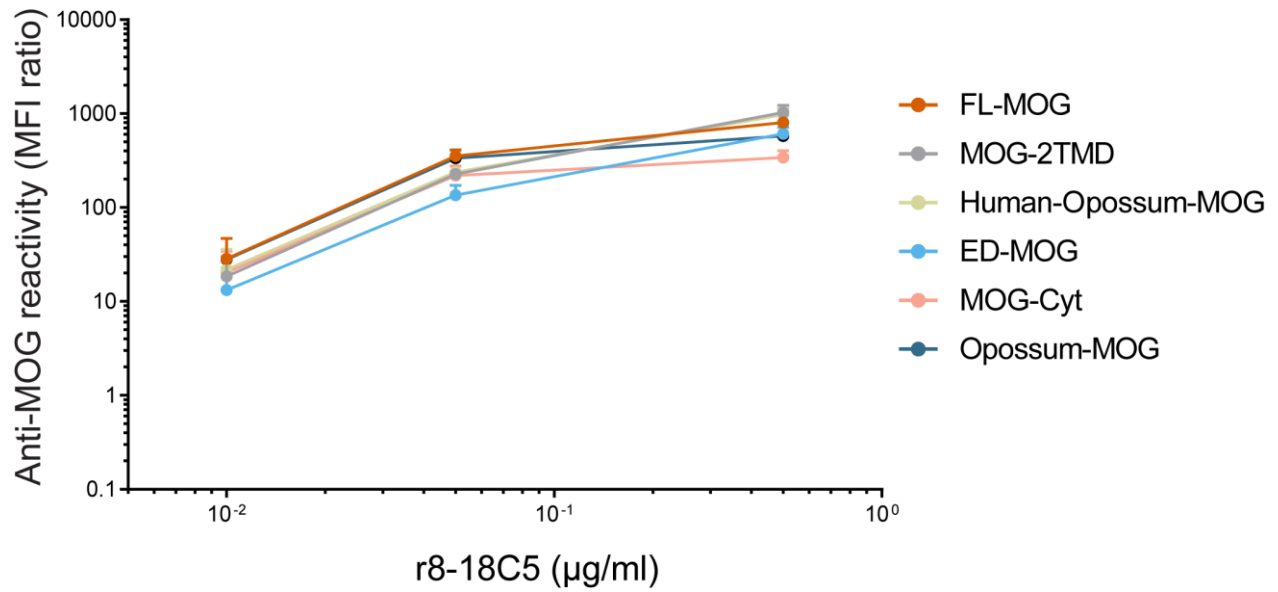
Suppl. Figure 3



Suppl. Figure 3: Individual responses of patients with MOG-Abs to different MOG variants quantified with two different gate settings. The serum response (diluted 1:50) of the analyzed patients to cells transfected with the indicated MOG-variants was determined. The anti-MOG response is given as MFI ratio as described in the materials and methods section and displayed here in a logarithmic scale. The mAb r8-18C5 and a control sample (C) were run in parallel. The mean + SEM of two experiments is shown. The horizontal grey dotted lines in **A**) and **B**) represent the cut-off used to determine MOG+ sera to FL-MOG and it is 2.27 (mean + 3SD of controls). Since the different MOG-variants were expressed in different intensities (details in **Suppl. Figure 2**), we used different gating strategies to take this into consideration. In **A**) cells

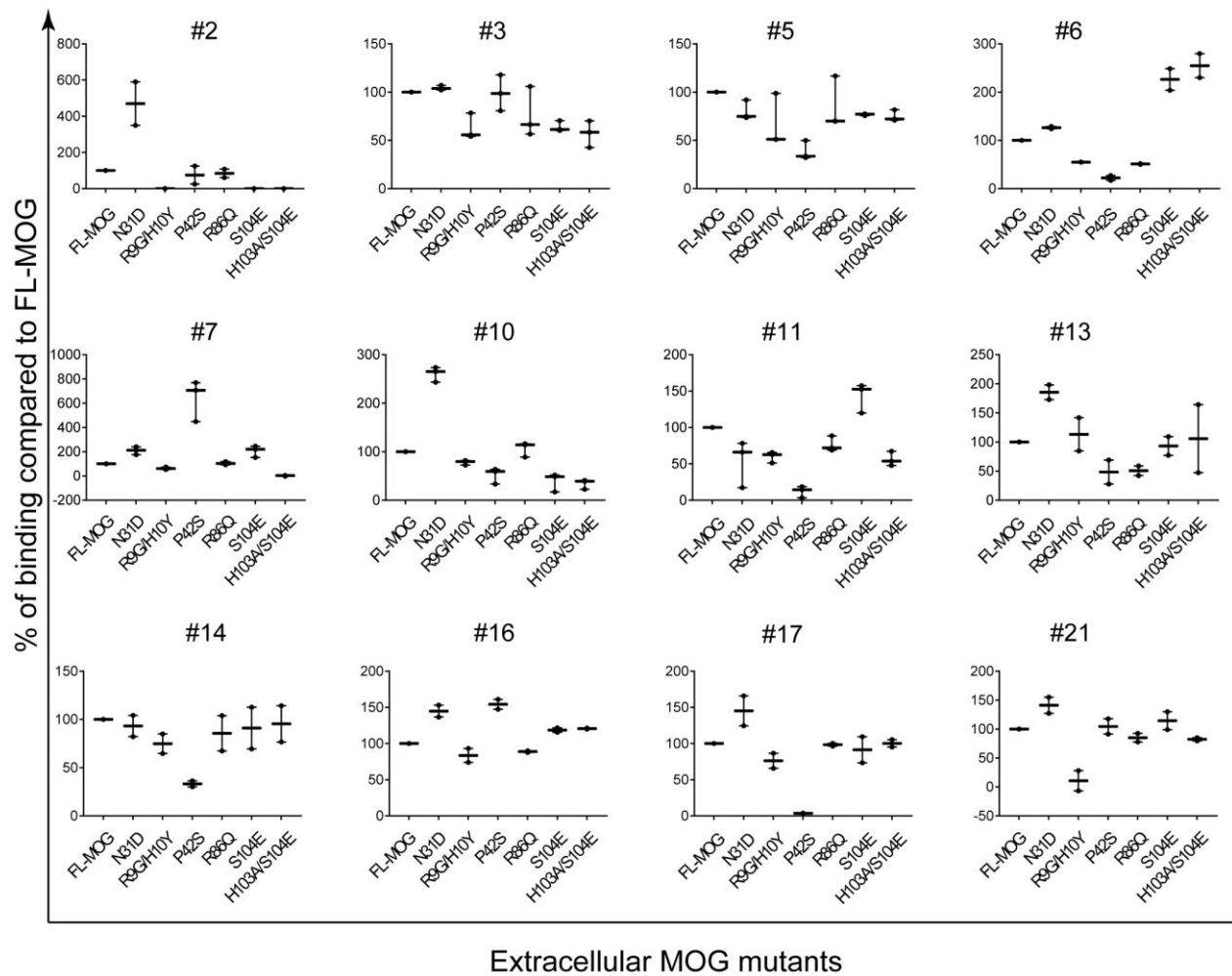
with an EGFP signal of 100-500 were included, in **B**) cells with an EGFP signal >100. While in most instances, the graphs in **A** and **B** look similarly, these two presentations provide complementary information in special instances. For example, for patient #22 the response to ED-MOG appears higher in **B**), but when considering the gates of 100-500, it becomes clear that this patient recognizes ED-MOG and FL-MOG similarly (**A**).

Suppl. Figure 4



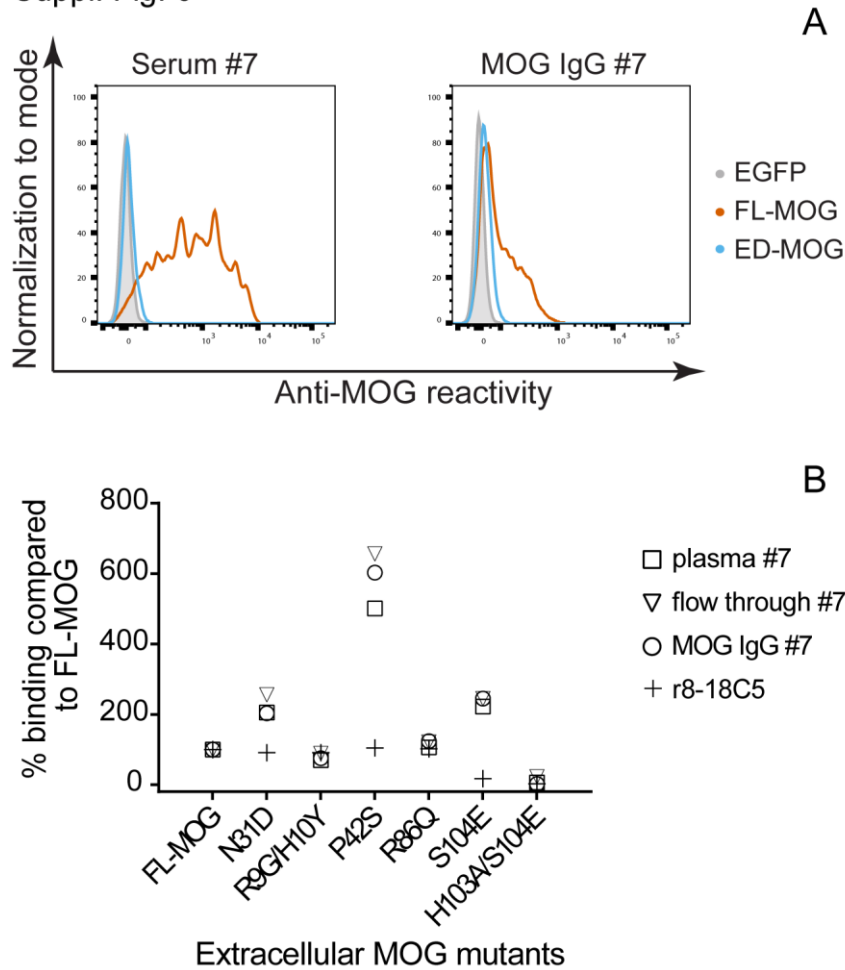
Suppl. Figure 4: Dose response of r8-18C5 on all the MOG variants. Increasing concentrations of r8-18C5 (0.01 $\mu\text{g/ml}$, 0.05 $\mu\text{g/ml}$ and 0.5 $\mu\text{g/ml}$) bound similarly to the applied MOG variants in this study. Cells with EGFP signal 100-500 were used in the analysis.

Suppl. Figure 5



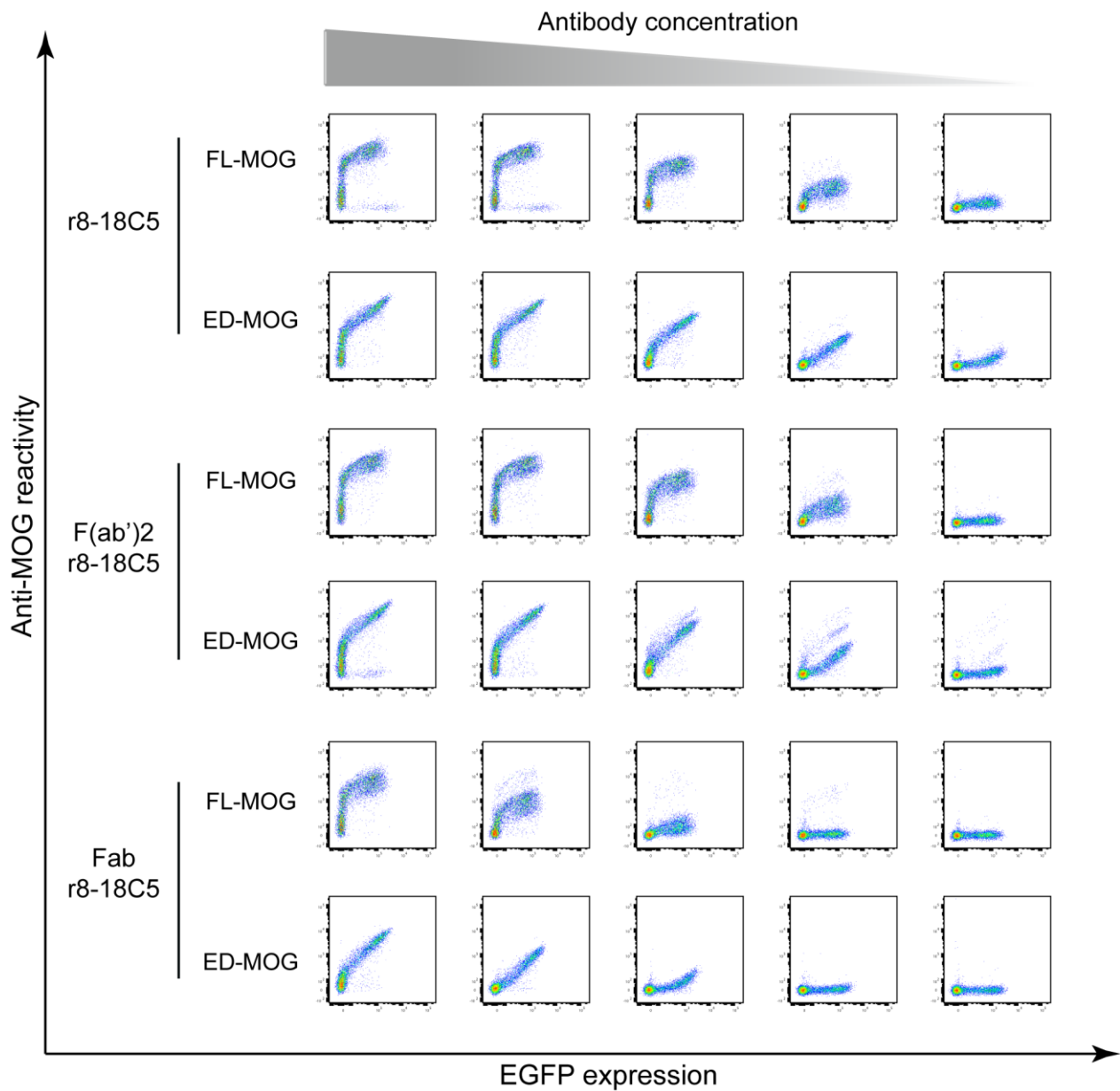
Suppl. Figure 5: Differential binding to mutants of the extracellular N-terminal part of MOG. The indicated MOG-variants were transiently transfected and the recognition by patients' sera in relation to wild type human MOG (described throughout the paper as FL-MOG) is given. Recognition of these mutants of patients #5 and #7 were also described in (Spadaro *et al.*, 2018), and of patient #24 in (Winklmeier *et al.*, 2019). Error bars indicate SEM of 2-3 experiments.

Suppl. Fig. 6



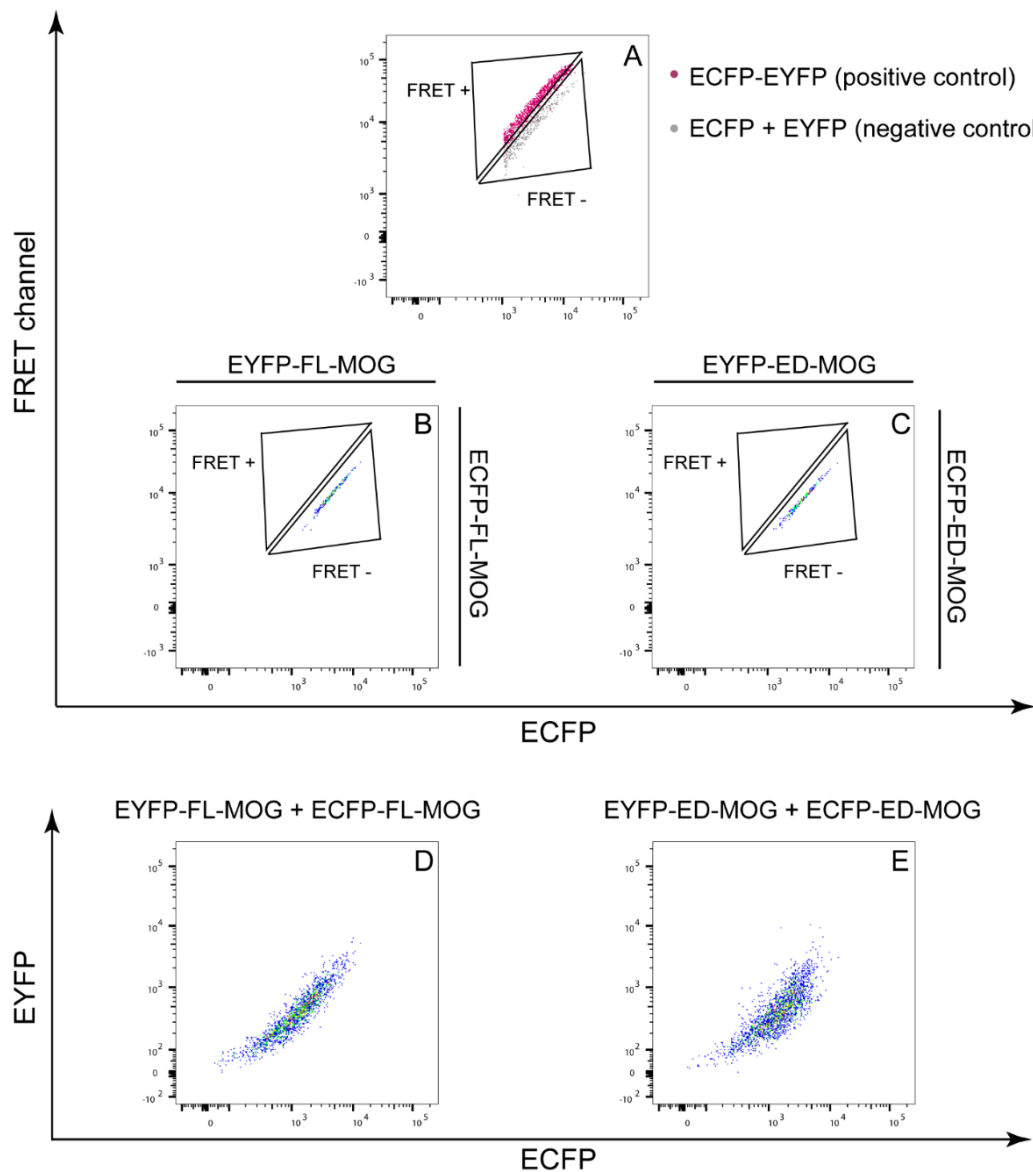
Suppl. Figure 6: MOG antibodies affinity-purified with MOG-1-125 compared with serum, plasma and flow-through. **A)** Serum (diluted 1:50) and MOG antibodies affinity-purified with MOG-1-125 (15 $\mu\text{g/ml}$), of patient #7 were tested for binding to cells transfected with FL-MOG or ED-MOG. **B)** Plasma (diluted 1:25), MOG antibodies affinity-purified with MOG-1-125 (15 $\mu\text{g/ml}$) and flow-through of patient #7 were tested also on cells transfected with extracellular mutants of MOG. The serum of this patient had a similar reactivity to the plasma towards the mutants (data not shown).

Suppl. Figure 7



Suppl. Figure 7: Recognition of FL-MOG and ED-MOG by F(ab')2 and Fab of r8-18C5. HeLa cells transiently transfected with FL-MOG or ED-MOG were tested for MOG-recognition with different concentrations of r8-18C5 and its F(ab')2 or Fab preparations at concentrations of 10 $\mu\text{g/ml}$, 1 $\mu\text{g/ml}$, 0.1 $\mu\text{g/ml}$, 10 ng/ml and 1 ng/ml .

Suppl. Figure 8



Suppl. Figure 8: Förster resonance energy transfer (FRET) shows no dimerization of MOG variants. **A)** The FRET+ control (ECFP-EYFP fusion construct in magenta) and the FRET- control (ECFP co-transfected with EYFP in grey) are shown. They define the FRET+ and FRET- gatings. **B, D)** HEK-293T cells were cells co-transfected with ECFP-FL-MOG together with EYFP-FL-MOG. **B)** FRET-signal. The cells localized in the FRET- gate, indicating no dimerization between FL-MOG molecules. **C, E)** HEK-293T cells were co-transfected with ECFP-ED-MOG and with EYFP-ED-MOG. **C)** FRET-signal. The cells localized in the FRET- gating, indicating that dimerization also does not occur between ED-MOG molecules. **D)** and **E)** Dot-plots show the expression intensity of EYFP-FL-MOG + ECFP-FL-MOG and of EYFP-ED-MOG + ECFP-ED-MOG.

Suppl. Figure 9

```

hMOG 1 MASLSRPSLPSCCLCSFLLLLLLQVSSSYAGQFRVIGPRHPIRALVGDEVELPCRISPGKN 60
mMOG 1 MACLWSFSWPSCFLSLL-LLLLQLSCSYAGQFRVIGPGYPICALVGDEAELPCRISPGKN 59
oMOG 1 MRNLPRSSLPGYLISFFFLFLLQLPSTYSYGQFRVIGQDHPTQAFVGGLIELSCHLSPAKN 60
      * * * * *
hMOG 61 ATGMEVGWYRPPFSRVVHLYRNGKDQDQDAPEYRGRTELLKDAIGEGKVTLRIRNVRF 120
mMOG 60 ATGMEVGWYRPPFSRVVHLYRNGKDQDAEQAPEYRGRTELLKETISEGKVTLRIRNVRF 119
oMOG 61 ATGMEIGWYRPPFSRVVHLYRNGKDQDAEQAPEYRDRTKLVKDAIGEGKVTLRIRNVRF 120
      *****
hMOG 121 DEGGFTCFRDHSYQEEAAMELKVEDPFYVWSPGVLVLLAVLPVLLQITVGLIFLCLQY 180
mMOG 120 DEGGYTCFFRDHSYQEEAAMELKVEDPFYVWNPVGLTIALVPTILLQVPVGLVFLFLQH 179
oMOG 121 DEGGYTCFFRDHSYQEEAAMQLKVEDPFYWLNHGILVLIAVLPILILQITIGLGLYMQH 180
      *****
hMOG 181 RLRGKLRAEIENLHRTFDPHFLRVPCWKITLFVIVPVLGPLVALIICYNWLHRRLAGQFL 240
mMOG 180 RLRGKLRAEIENLHRTFDPHFLRVPCWKITLFVIVPVLGPLVALIICYNWLHRRLAGQFL 239
oMOG 181 RLRGKLQAEIENLHRTFDPYFLRVPCWKIALFVIVPVLGPLAAMIICYNWLHRRLAGQFL 240
      *****
hMOG 241 EELRNPF 247
mMOG 240 EELRNPF 246
oMOG 241 EELKYPF 247
      *** **

```

Suppl. Figure 9: Comparison of sequences of MOG from human (hMOG), mouse (mMOG) and opossum (oMOG). The first and second hydrophobic domains are highlighted in grey. The amino acids in or around the second transmembranous domain that, according to our model (**Figure 7**) are involved in kinks and cytoplasmic localization of the C-terminus, are in bold.